Nonlinear Dynamics and Fractal Avalanches in a Pile of Rice

Rinke J. Wijngaarden[1], Kinga A. Lőrincz[2], and Christof M. Aegerter[3]

[1] Division of Physics and Astronomy, Faculty of Sciences, Vrije Universiteit, De Boelelaan 1081, 1081HV Amsterdam, The Netherlands
rw@nat.vu.nl

[2] Division of Physics and Astronomy, Faculty of Sciences, Vrije Universiteit, De Boelelaan 1081, 1081HV Amsterdam, The Netherlands
ka.lorincz@few.vu.nl

[3] Division of Physics and Astronomy, Faculty of Sciences, Vrije Universiteit, De Boelelaan 1081, 1081HV Amsterdam, The Netherlands
present address:
Fachbereich Physik, Universität Konstanz, Universitätstrasse 10, P.O. Box 5560, D-78457 Konstanz, Germany
christof.aegerter@uni-konstanz.de

1 Introduction

The result of a measurement x e.g. of the length of Dutch men or the weight of rice grains is usually Gaussian distributed with a well-defined average $\bar{x}$ and width σ. Quite to the contrary, around 1944 Gutenberg and Richter [1] discovered that the size of earthquakes follow a power law distribution: an earthquake of energy E has a probability to occur given by

$$P(E) \sim E^{-\tau} \tag{1}$$

where τ is close to 1. Such power law behaviour is quite special since an average and width cannot be defined. A particularly nasty property is that the probability decays only as a power law, while in the Gaussian case it decays faster than exponentially. As a result there is a non-negligible chance for a huge earthquake.

Many systems in nature display dynamics dominated by similar punctuated behaviour, which we call here generically 'avalanches'. Other examples are: snow-avalanches [2], forest fires, rain fall [3], stock-market indices [4] and the extinction of species in biology [5]. In all these cases, due to a power law distribution function, there is a finite chance for very big, catastrophic events.

In 1988, Bak, Tang and Wiesenfeld [6] introduced the Self-Organized Criticality (SOC) model; it was made accessible for a broad audience by the book "How Nature Works" [7]. In fact, apart from the power law behaviour, there are now many more criteria [8] for SOC behaviour, which enable a more stringent test.

Although there has been a very significant amount of numerical simulations on SOC systems, there are only very few controlled experimental

investigations. Up to now experimental work was much hampered by the difficulty to determine whether a particular system is SOC or not. In fact, for sand piles both SOC and non-SOC behaviour has been reported [9] (based on power law scaling of avalanches only).

We study experimentally a 3-dimensional pile of rice with a 1×1 m^2 floor area. Using the more stringent criteria, we discovered [10] that rice behaves as SOC: not only is the avalanche distribution a power law, but also finite size scaling (FSS) is obeyed: the maximum avalanche size scales in a particular manner with the size of the system, as predicted by SOC-theory. We determine the exponent (power) of the power law distribution function as well as the fractal dimensions of the avalanche cluster (avalanche exponents). On the other hand, we also determine the growth and roughness exponents (surface exponents) for the rough surface that remains after many avalanches. SOC theory does not fix the exact values of the individual exponents, but does predict scaling relations e.g. between the avalanche and surface exponents. We find that as far as we tested these relations, they are obeyed for our experimental data.

In addition, SOC theory predicts that a system which is not yet 'critical' moves in a particular manner toward the SOC state described by the so-called gap-equation. This approach is characterized by another exponent, the value of which, interestingly, is given through another scaling relation containing only values for the SOC state [11]. Also this relation is obeyed for our pile.

After introducing our experimental set-up, we review these ideas and corresponding experimental work in more detail below. We conclude by some (experimentally tested) ideas on how to prevent big catastrophes.

2 Experiment: A Big Rice Pile

For the experiments we use long grained rice with dimensions of typically $2 \times 2 \times 7$ mm^3, similar to rice A of [12]. Our experimental set-up is shown in Fig. 1. It consists of a rice pile of 1×1 m^2 floor area on the top of which rice rains down from a linear source. Uniformity within 5% in the distribution along this line is guaranteed by the use of a distributor board, see Fig. 2.

By the distributor board the stream of rice is continuously split such that at the bottom we end up with a row of 64 uniformly distributed sub-streams. A plastic flap at the bottom is used for further spreading and to slow down the rice before it impinges onto the surface of the pile.

To rain down at a uniform rate, the rice is fed to the distribution board from a mechanically stirred funnel, from which the rice emerges at an approximately constant rate of typically 1500 grains per image (taken at 30 s interval), distributed over the whole width of the distributor board.

To monitor the shape of the pile as function of time, a set of coloured (red, green and blue) lines (see Fig. 3) is projected onto the pile using an overhead projector. Photographs are taken from a different viewpoint with

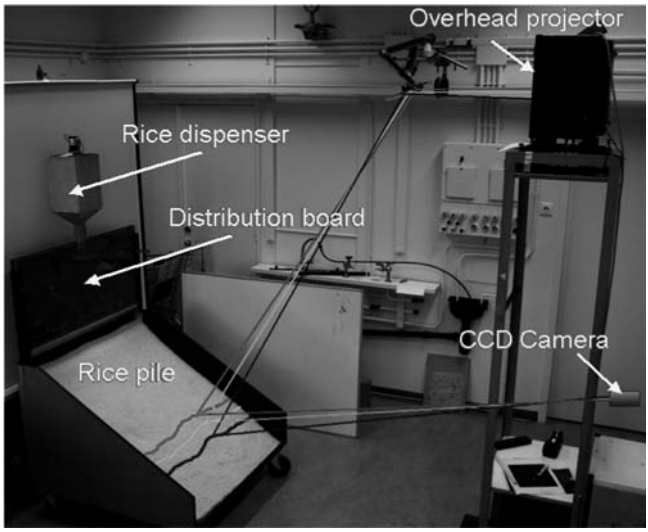

Fig. 1. The rice set-up with 1×1 m^2 floor area. Rice rains down from the distributor board onto the top of the pile. The 3-dimensional shape of the pile is reconstructed from the shape and position of a set of coloured lines projected onto the pile

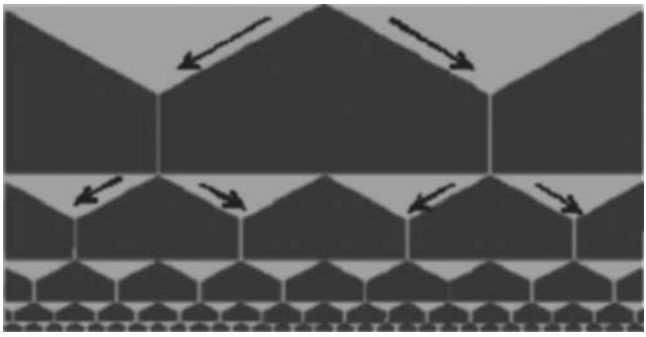

Fig. 2. The binary distributor board used to create a uniform line source

respect to the projector, such that the shape of the pile can be reconstructed using the geometry of stereoscopy.

Typically an experimental run lasts 4 hr, with a picture being taken every 30 s. The pictures are taken with a digital camera with a resolution of 2048×1536 pixels. For each picture the centre of gravity of each line is detected (see Fig. 3, lower panel), from which the 3-dimensional surface is reconstructed. From the 3-dimensional surfaces, the roughening properties (see Sect. 3 below) and the avalanche properties (see Sect. 4 below) are calculated.

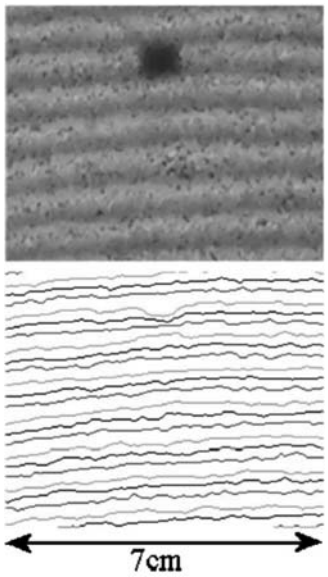

Fig. 3. (Top panel) detail of the set of coloured lines projected onto the pile. (Bottom panel) the centre of gravity of the lines as recognized by the software

3 The Rough Surface of the Pile

The surface of the rice pile is not completely smooth, but shows surface fluctuations, which are mainly due to the occurrence of avalanches that remove material from a more elevated part of the pile and deposit it at a lower position. Since the avalanches have all kinds of sizes, they lead to surface fluctuations of all kinds of size.

A common way to analyze such 'rough' surfaces is to consider the spatial and temporal dependences of the root-mean-square (RMS) 'width' of the surface. For this we first fit a plane $\bar{h}(x,y,t)$ to the surface $h(x,y,t)$ of the pile. The RMS deviations $w(L,t)$ of the surface with respect to this plane are then easily calculated from

$$w(L,t) = \left(\frac{1}{L^2} \sum_{x,y=1}^{L} \left[h(x,y,t) - \bar{h}(x,y,t) \right]^2 \right)^{\frac{1}{2}} . \tag{2}$$

It is well known [13], that initially this width grows as a power law of time $w(L,t) \sim t^{\beta}$ where β is called the growth exponent, while at later times, when lateral correlations span the whole size of the system L, this width grows as a power law of system size $w(L,t) \sim L^{\alpha}$ where α is called the roughness exponent. Hence the exponents α and β can be obtained from the slope in a log-log plot of w vs. L and t respectively, see Fig. 4. In fact, a

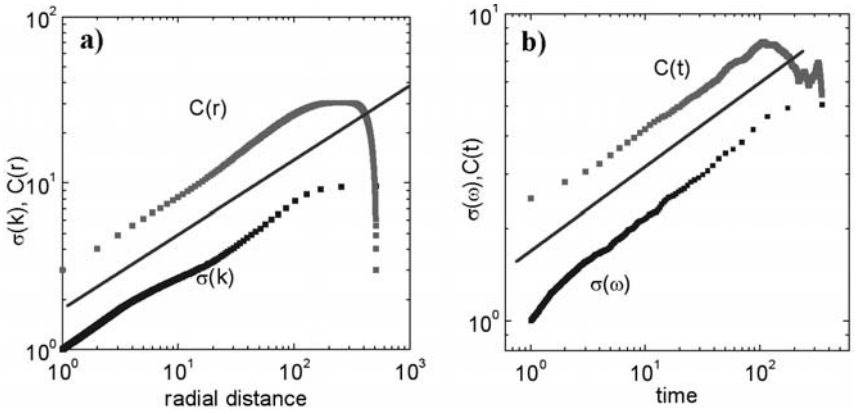

Fig. 4. (**a**) Determination of the roughness exponent from the spatiotemporal correlation function $C\,(L,0)$ and the distribution function $\sigma\,(k)$ as defined in the text. The line indicates the average slope, which defines the value for the roughness exponent obtained. (**b**) Determination of the growth exponent from the spatiotemporal correlation function $C\,(0,t)$ and the distribution function $\sigma\,(\omega)$ as defined in the text. The line indicates the average slope, which defines the value for the growth exponent obtained

more accurate way to determine these exponents was used for this figure. It is based on the correlation function

$$C\,(L,t) = \left(\langle [h\,(x+\xi, y+\eta, t+\tau)\;\; h\,(\xi,\eta,\tau)]\rangle_{L,\tau}\right)^{\frac{1}{2}} \tag{3}$$

where the $\langle\cdot\rangle_\tau$ indicates averaging over all $\tau > 0$, and where $\langle\cdot\rangle_L$ indicates averaging over all points (ξ,η) and all (x,y) at a radius L from the origin. The behaviour of this correlation function is similar to that of the width i.e. $C\,(0,t) \sim t^{\beta}$ and $C\,(L,0) \sim L^{\alpha}$. Alternatively [14], one may also start with the radially averaged power spectrum $S\,(k)$ of the surface defined by

$$S\,(k) = \left|\hat{h}\,(k_x, k_y)\right|^2 \tag{4}$$

where $\hat{h}$ denotes the 2-dimensional Fourier transform of the surface and $k^2 = k_x^2 + k_y^2$. The corresponding spatial distribution function $\sigma\,(k)$ behaves in the same manner [14] as the correlation function $C\,(x,t)$ where

$$\sigma^2\,(k) = \int_0^k S\,(\kappa)\,\kappa\;\mathrm{d}\kappa\;. \tag{5}$$

Similar relations are defined for the temporal distribution function $\sigma\,(\omega)$. In Fig. 4 we show this scaling behaviour.

The resulting exponents are $\alpha = 0.42(3)$ for the roughness exponent and $\beta = 0.28(3)$ for the growth exponent. Before discussing these values, we shall now turn our attention to the avalanche behaviour.

4 Avalanches on the Rice Pile

A typical avalanche is shown in Fig. 5. The size and shape of the avalanches can be determined from the height difference of the surface between two consecutive images. In this manner we determine the size of the avalanches (as a volume, which can be expressed in the number of rice grains participating) and also the shape of the avalanches. In particular, we determine the fractal dimension D of the avalanche cluster and also the fractal dimension d_B of the area on which the avalanche happened: this area is a projection of the avalanche shape on the surface of the pile. Both fractal dimensions are determined using box counting [15].

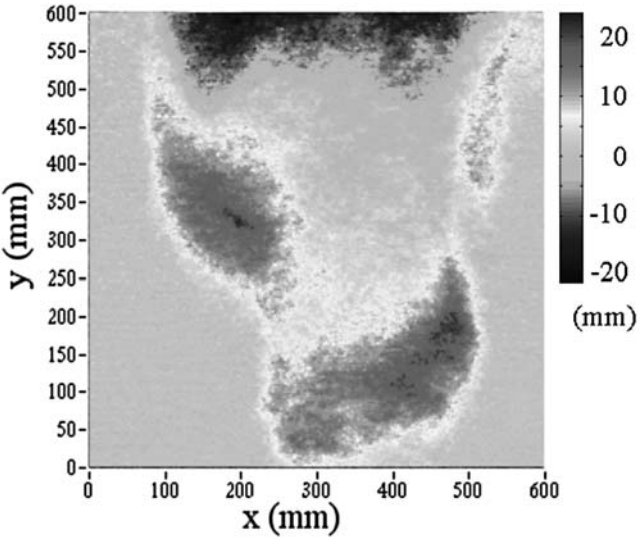

Fig. 5. Typical avalanche on the rice pile. The picture shows the avalanche as the difference in height between two successive images

A plot of avalanche size as a function of time, presented in Fig. 6, clearly shows the punctuated behaviour.

The avalanches were determined in the central part of the pile with a size of 600×600 mm^2. In Fig. 7a we plot the size distribution for the avalanches in this area, but also for subsets of this area.

We observe power law behaviour with a size distribution exponent $\tau = 1.21\,(2)$ (corresponding to the straight line), but clear deviations from this behaviour occur above a certain size, which is related to the size of the area of observation. Interestingly, SOC-theory makes a precise prediction for this deviation: it occurs because the avalanche 'feels' the size of the system L, i.e. because the linear size of the avalanche becomes comparable to L. Clearly

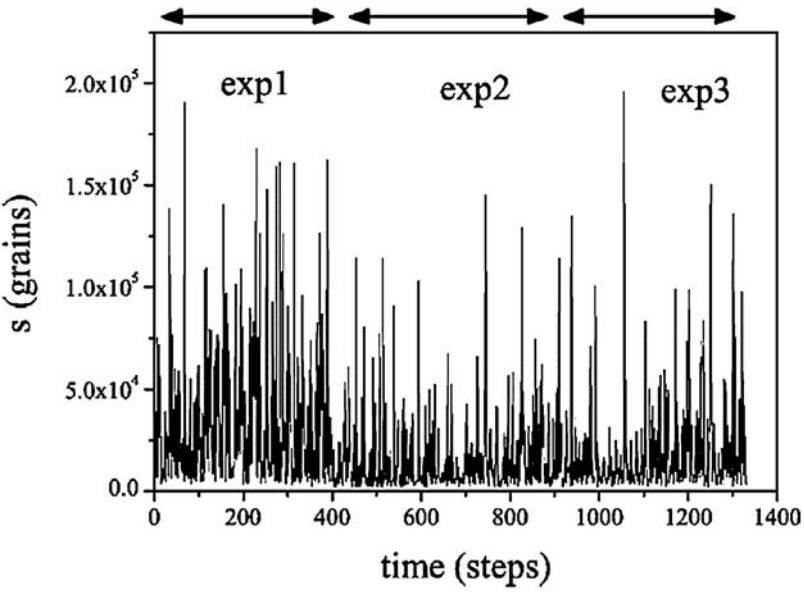

Fig. 6. Size of the avalanches as a function of time in the steady state, i.e. after the system has been left running for a long time. Results for three experiments are shown. Note the punctuated behaviour

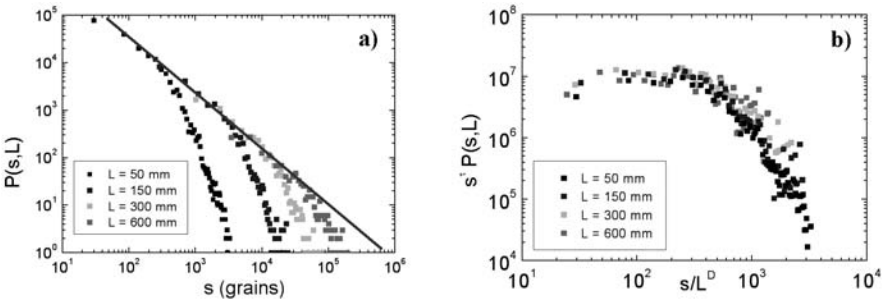

Fig. 7. (**a**) Size distribution of the avalanches. $P\,(s, L)$ is the number of avalanches of size s that were observed while monitoring a window of size $L \times L$ (**b**) Finite size scaling of the size distribution of the avalanches. Note the nice data-collapse: the deviation from power law behaviour starts from a size $s \sim L^D$ where D is the fractal dimension of the avalanche volume

this happens for $s \approx L^D$ and hence the deviation should scale with s/L^D. This is verified in Fig. 7b , where, in addition, the vertical axis was multiplied by s^τ to take out the power law. Clearly a very nice data-collapse is observed confirming the "finite size scaling"-prediction of SOC theory. This data collapse yields an accurate value for the exponents: $D = 1.99\,(2)$ and $\tau = 1.21\,(2)$.

5 Relation Between Avalanches and Surface

An avalanche disturbs and changes the surface on which it occurs and intuitively one might expect that there exists a relation between the properties of an avalanche and the surface that remains after the avalanche has taken place. On the other hand, avalanches are quite different from granular piles, and hence a comparison is not trivial. Below we discuss two relations between the statistical properties of avalanches and the surface that they leave behind. Subsequently, we verify whether these are obeyed in our experiments.

The first and most simple scaling relation is found by calculating the volume of a (fractal) avalanche. By definition, this volume is L^D since D is the fractal dimension of the avalanche cluster (which can be determined directly in our experiment). On the other hand, the volume should also be equal to the fractal surface times the fractal height. The fractal surface area is the projection of the avalanche cluster on an average (flat) plane trough the pile surface. The area of this projection is by definition L^{d_B} where d_B is the surface fractal dimension of the avalanche cluster, which can be easily obtained in our experiment. The height or thickness of an avalanche is obtained by subtracting the heights (in the direction perpendicular to the average plane, mentioned above) of the piles before and after the avalanche. Since the avalanche modifies the pile only locally, this fractal thickness scales as the surface roughness and is proportional to L^α. Combining these ingredients yields $L^D \sim L^{d_B} L^\alpha$ from which we obtain the scaling relation

$$D = d_B + \alpha \, . \tag{6}$$

The second scaling relation follows from the fact that the deviation from power law behaviour seen in Fig. 7 occurs because avalanches above a certain size 'feel' that the pile is finite. We shall now make this more explicit.

As stipulated above, the time evolution of an initially flat surface subject to roughening is such that at short times its root-mean-squared width w increases with time as $w \sim t^\beta$. After some time, however, lateral correlations extend over the whole area of the pile and w does not increase anymore: it is limited to a pile-size dependent value $w \sim L^\alpha$, where L is the linear size of the pile and α is the roughness exponent. At the cross-over time $t_\times$, both relations hold from which

$$t_\times \sim L^{\alpha/\beta} \, . \tag{7}$$

On the other hand, since this cross-over is due to correlations that start to span the whole system, $t_\times$ is also the moment when the first avalanche occurs that spans the whole pile; by definition the size of this avalanche is $s_\times$. Since we seed the pile with a constant rate, $t_\times$ also is proportional to the amount of mass M we must add to the pile to obtain such a pile-spanning avalanche. However, before we create an avalanche of size $s_\times$, many smaller avalanches have occurred, adding to the amount of material that we have to add before a pile-spanning avalanche takes place. Thus the total mass M is

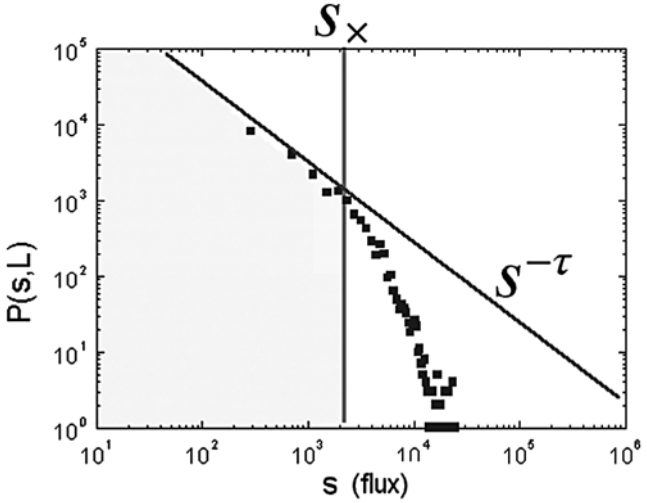

Fig. 8. The scaling relation $D\,(2-\tau) = \alpha/\beta$ is derived by comparing the time needed for correlations to span the whole pile and the time needed to create avalanches that span the whole pile (see text)

equal to the integral of the size distribution function up to $s_\times$, i.e. the shaded area in Fig. 8. This gives

$$t_\times \sim M = \int_0^{s_\times} sP\,(s)\,\mathrm{d}s \sim \int_0^{s_\times} s\; s^{-\tau}\mathrm{d}s \sim s_\times^{2-\tau}\;. \tag{8}$$

In the finite size scaling analysis we found that $s \sim L^D$, hence we obtain

$$t_\times \sim s_\times^{2-\tau} \sim L^{D(2-\tau)}\;. \tag{9}$$

Combination with (7) yields the exponent relation

$$D\,(2-\tau) = \frac{\alpha}{\beta}\;. \tag{10}$$

Equations (6) and (10), which were previously derived by Paczuski et al. [8], offer an interesting possibility: one can calculate the roughness and growth exponents, α and β, from the *avalanche* properties only. In the table below we compare the values [10] from such an analysis with those obtained above from a direct roughness analysis of the surface of the pile:

	α	β
from roughness analysis	0.42 (3)	0.28 (3)
from avalanche analysis	0.41 (3)	0.26 (2)

Clearly, an excellent agreement is found, which supports the underlying assumption i.e. that SOC theory yields a valid description of the avalanche behaviour in our pile.

It is interesting to note that the values we find for the roughening of our rice pile are very close to those observed for Kardar-Parisi-Zhang [16] (KPZ) systems. For a 2-dimensional interface it was found from simulations that for KPZ systems $\alpha = 0.39$ and $\beta = 0.24$, rather close to the values given in the table above. In addition, if we consider the roughening of contour lines (lines of equal height) on our pile, we find for these 1-dimensional interfaces $\alpha = 0.48\,(3)$ and $\beta = 0.33\,(3)$, while it can be shown [13] rigorously that for 1-dimensional KPZ $\alpha = 1/2$ and $\beta = 1/3$. Strangely enough, our system is very unlike a KPZ system: the latter is governed by a Langevin (differential) equation, which describes the development of the interface in a deterministic and local fashion (although the effects of disorder are very important and must be included in the description). To the contrary, our system seems much more random and non-local due to the occurrence of avalanches. Nevertheless the most likely manner of change of our pile is by increase or decrease of its height, which is most easy in a direction that is parallel to the local normal to the surface. Exactly this is also the main ingredient in the derivation of the KPZ equation: growth always proceeds along the local normal. Possibly, the KPZ model extends to non-Langevin systems obeying this same growth rule.

6 Avalanches as Spatiotemporal Fractals

In this section we discuss the spatiotemporal structure of the avalanches. It is quite natural under our condition of constant seeding of the pile, to consider all avalanches together as belonging to one superavalanche, which is punctuated in time. In fact, using similar theoretical ideas as above, one can make a testable prediction for the power spectrum of this superavalanche.

To derive a scaling relation for the avalanche power spectrum exponent, let us consider the development of an avalanche, see Fig. 9. Shown are five successive stages of the development of an avalanche cluster, which is shown full-grown at the top. At the bottom of the figure, the substrate area of this avalanche is shown. At a certain moment during the avalanche a site is changed (indicated in the middle three pictures by a red colour) or not (blue). If we consider a single site, then the behaviour as a function of time is punctuated and a time-line through such a site (indicated by the vertical line) is a fractal. We define the length of this time-line as T^θ where T is the total time needed to create the full-grown avalanche and θ is the fractal dimension of the time-line (to be calculated below). If the linear size of the full-grown avalanche cluster is L (note the change in definition of L), then (according to similar arguments as given above concerning $t_\times$) the time needed to create such correlated cluster is $T \sim L^{\alpha/\beta}$. Hence the length of the time-line is $T^\theta \sim L^{\theta\alpha/\beta}$. The full-grown cluster is created during the time T and has a volume that is easily calculated from its substrate area L^{d_B} and its height, corresponding to the number of times T^θ that activity occurred during its

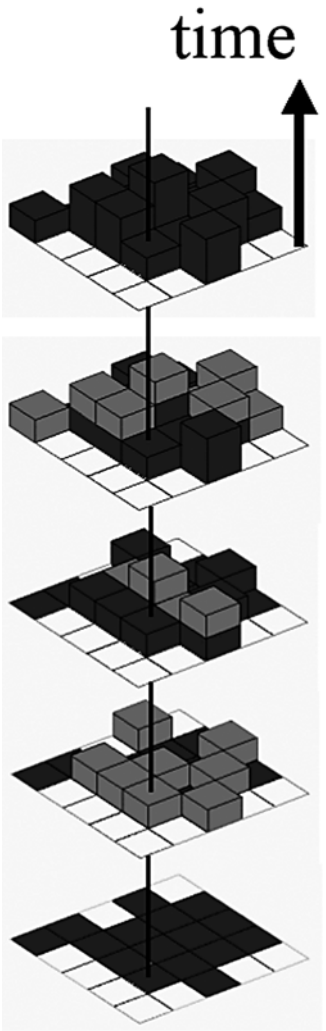

Fig. 9. Schematic representation of the spatiotemporal structure of an avalanche. Shown are five successive stages of development of an avalanche cluster, shown in full-grown state at the top. At the bottom the substrate area of the full-grown avalanche is shown. As time progresses there is activity (grey) or not (black) at a particular site. A time line running through one site is indicated by the vertical line. For further explanation see text

growth. From this we obtain for the volume of the full-grown avalanche cluster $V = L^{d_B} \times L^{\theta\alpha/\beta}$. On the other hand, this size is also L^D, since D is the fractal dimension of the full-grown avalanche. Combining yields the scaling relation

$$D = d_B + \theta \frac{\alpha}{\beta} \,. \tag{11}$$

Solving this for θ yields

$$\theta = (D - d_B) \frac{\beta}{\alpha} = \beta \tag{12}$$

where we have used (6). Hence the fractal dimension of the time line through a single site has the same value as the growth exponent.

We now determine the consequence for the power spectrum. Consider first the activity-function $A(t)$ for a certain timeline, such as in Fig. 9. $A(t)$ is one at each moment of activity and zero at all other times. On the average the total number of ones of A during a time t, which we call $n(t)$ is given by

$$n(t) = \int_0^t A(\tau)\, \mathrm{d}\tau \sim t^{\beta} \tag{13}$$

since the number of points on a length t of time-line with fractal dimension β is given by t^{β}.

By definition, the temporal correlation function for the avalanche is $C(t) = \langle A(\tau) A(\tau + t) \rangle_{\tau}$ (note that this $C(t)$ for activity during avalanches is different from the $C(t)$ calculated above for rough surfaces), where the average is over all starting times τ and all time lines. In this context, $C(t)$ is also called [8] the all-return probability $P_{\mathrm{all}}(t)$ i.e. the probability for a site that is active at $\tau = 0$ to become active again at $\tau = t$. Hence [8] on the average $n(t+1) = n(t) + C(t)$. Thus

$$C(t) \sim \frac{dn(t)}{dt} \sim t^{\beta - 1} \,. \tag{14}$$

And for the power spectrum [17]:

$$S(f) \sim f^{-\beta} \,. \tag{15}$$

An experimental power spectrum is shown in Fig. 10. The red line indicates power law behaviour with a negative power of $0.27\,(3)$. According to (15) one expects a value equal to the growth exponent $\beta = 0.28\,(3)$ as determined above. Clearly we find a good agreement supporting again the applicability of SOC theory.

7 How to Prevent Avalanches

It is rather worrying that despite vigorous efforts to prevent snow avalanches by controlled explosions, accidents still occur. In fact, the same applies to forest fires (notably in the National Parks in the US), where 'controlled' burning sometimes gets out-of-hand and starts large fires. In fact, it is a

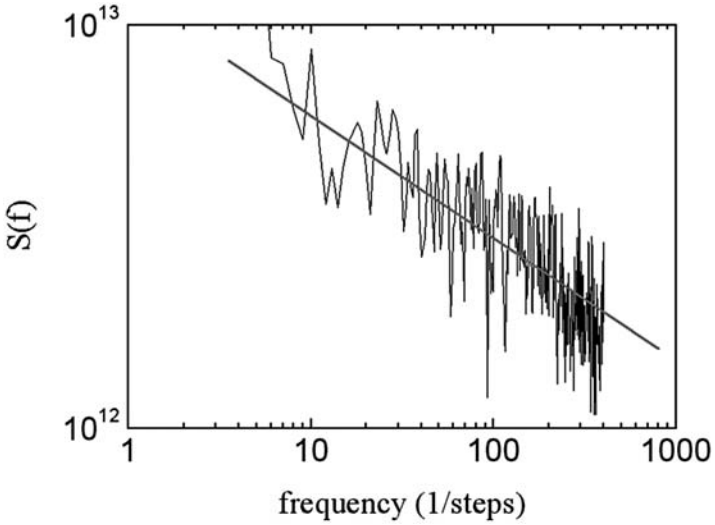

Fig. 10. Power spectrum of the avalanches of Fig. 6. The red line indicates power law behaviour with a negative power of 0.27 (3) , very close to the value of the growth exponent, 0.28 (3) , in good agreement with SOC theory

property of SOC that 'small' disturbances may lead to big avalanches, making control very difficult.

In Fig. 11 we replot the data of a comparative study [2] of snow avalanches in two regions of the US, one where controlled explosions were used to try to prevent the occurrence of large avalanches and another, where no explosions were made. Clearly, the power law distributions are very similar, with nearly equal slope. The disturbed region shows even slightly worse behaviour: the sizes are slightly larger and the decay is slightly slower, making large avalanches relatively more likely.

To investigate another method for the prevention of devastating avalanches, we study the *transient* state. This is the state of the system before it reaches criticality. The rice pile was prepared manually to be at an angle much smaller than the critical angle (we refer to this state hereafter as 'flat'), after which the measurement was immediately started. A detailed analysis of the multi-scaling properties of the temporal correlation function was made [18], but here we shall concentrate on the avalanche properties.

The punctuated behaviour of the avalanches is shown in Fig. 12, where we see that initially large avalanches do not occur. Indeed averaging the avalanche sizes over 100 consecutive time-steps shows a linear increase with time, see Fig. 13, while the system is moving from the prepared 'flat' state towards steady-state SOC behaviour.

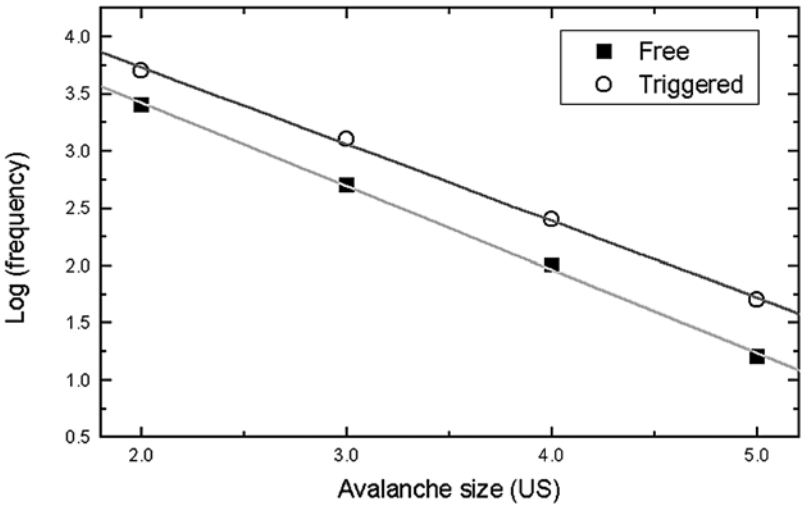

Fig. 11. Replot of the data of Birkeland and Landry [2], showing that the avalanche size distribution for snow avalanches is slightly 'worse' for the region where attempts were made to prevent large avalanches by controlled explosions

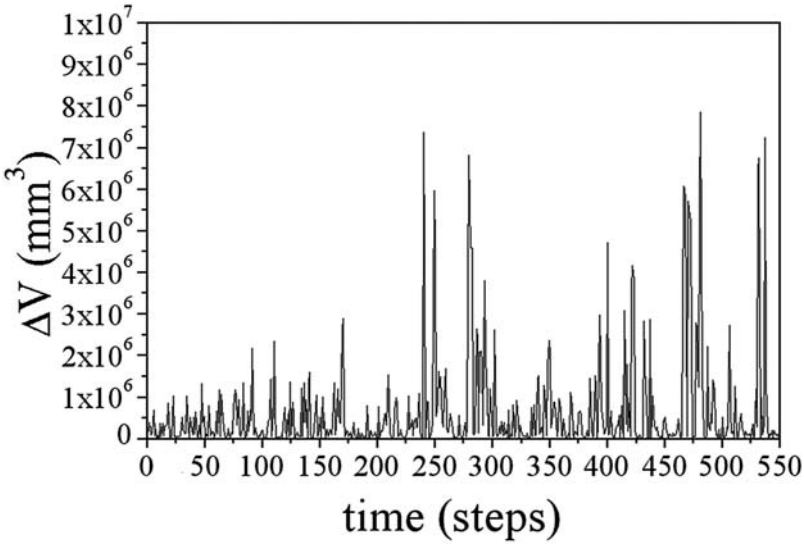

Fig. 12. Avalanche volume versus time immediately after preparing the pile manually in a rather flat state. Clearly, in the beginning large avalanches do not occur

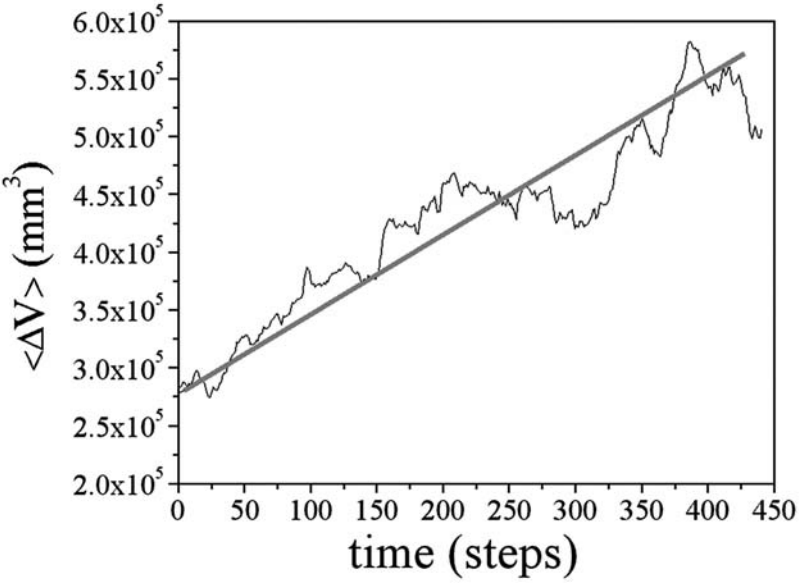

Fig. 13. Size of the avalanches of Fig. 12 averaged over 100 time steps. Clearly the average avalanche size increases linearly with time while the system is developing towards the SOC steady state

Interestingly, SOC theory [8] prescribes how the system should approach the SOC state. We call the critical slope of the rice f_c. This is the maximum slope that a rice pile can have without starting to slide. The value $f_c = 0.92\,(1)$ was determined experimentally [11] (i) by slowly tilting a small box with rice until it started to slide and (ii) from the maximum slope observed anywhere in our large pile during many experiments.

We call the maximum slope observed anywhere in the pile at a certain instant in time G. SOC theory describes how G approaches f_c after starting from a 'flat' state. In particular, it predicts that the average avalanche size $\langle \Delta V \rangle$ diverges as the SOC state is approached according to $\langle \Delta V \rangle = (f_c - G)^{-\gamma}$. Combining this with the experimental observation that $\langle \Delta V \rangle \sim t$ yields

$$f_c - G \sim t^{-1/\gamma} \,. \tag{16}$$

Indeed, from the experimental data we find a reasonable agreement to this behaviour, see Fig. 14, except for the very beginning of the experiment.

In fact, according to SOC theory [8,11], the observed power $1/\gamma$ is given by

$$\frac{1}{\gamma} = \frac{1 + d_B/D - \tau}{2 - \tau} \,. \tag{17}$$

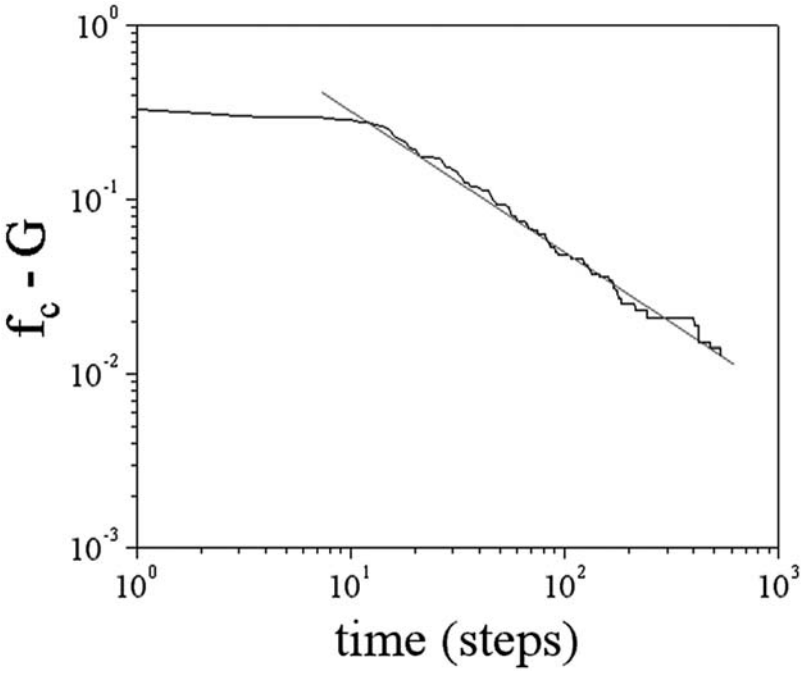

Fig. 14. Difference between actual maximal slope anywhere in the pile G and the critical slope f_c of rice as a function of time. The red line indicates power law behaviour with slope 0.8 (1)

This is an interesting relation, because it connects the behaviour in the transient non-SOC state as given by γ to exponents (D, d_B and τ) of the steady SOC state. Experimentally, we find $1/\gamma = 0.8\,(1)$, while using the values obtained above for D, d_B and τ, one would expect $1/\gamma = 0.74\,(2)$, which is a nice agreement.

In addition to the change in average avalanche size, also the avalanche size distribution exponent τ changes during the transient state, see Fig. 15. Initially τ is larger, indicating a faster decrease of the distribution function with increasing avalanche size and hence a smaller chance for large avalanches. This makes the transient state safer. An alternative to firing explosives in (near-)critical snow masses is to disturb the snow at an early stage. Thus the snow may be kept from developing SOC behaviour. In addition, due to the larger τ in the transient, even if triggering provokes an avalanche, the chances that it is very big are significantly reduced. Similar arguments hold for controlled burning in the prevention of forest fires.

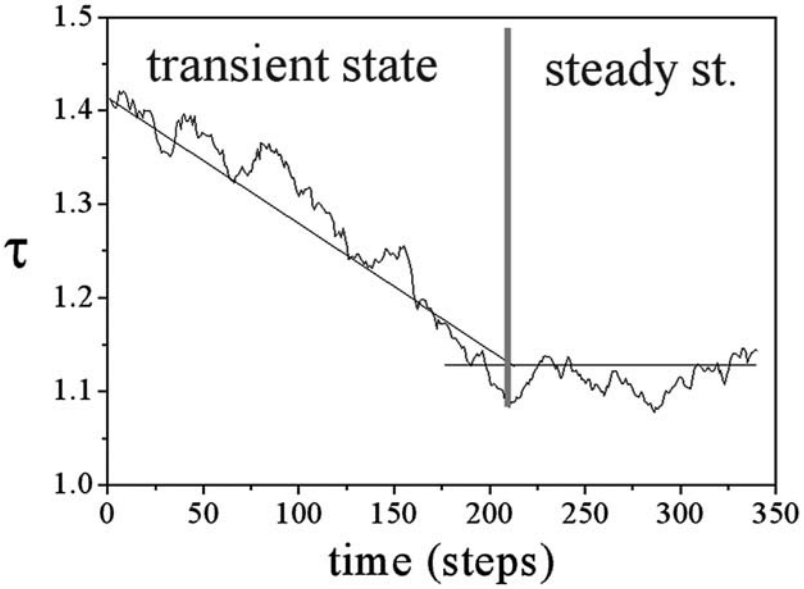

Fig. 15. Change of the avalanche size distribution exponent τ as a function of time in the transient state. Clearly at early times the distribution function is steeper, making large avalanches less likely

8 Conclusions

Self-organized criticality is a class of models meant to describe punctuated behaviour in naturally occurring phenomena such as earthquakes, avalanches and extinctions of species in biology. These wildly different phenomena have characteristic properties, such as the size of events, that all have power law distribution functions. The exponents of these power laws may vary from system to system, however, SOC theory [8] gives explicit relations between the exponents. In fact, many of the exponents can be expressed in terms of only three of them: D, d_B and τ.

We have experimentally investigated the statistical properties of avalanches on a 3-dimensional pile of rice and find that avalanche sizes are indeed power law distributed. In addition, we find that the starting point for deviations from power law behaviour scales as $s_\times \sim L^D$, as predicted by SOC theory. Using this and direct imaging of the avalanches, we have directly measured D, d_B and τ. From the properties of the surface of the pile, we independently determined its roughness and growth exponents α and β. We have thus verified that within experimental accuracy, the scaling relations $D = d_B + \alpha$ and $D\,(2 - \tau) = \alpha/\beta$ are obeyed.

In addition, we have verified that the value of the exponent of the power spectrum of the avalanches is equal to β as predicted by another scaling relation.

It is striking that, while we find SOC behaviour in our rice pile and are thus able to verify the exponent relations proposed by Paczuski et al. [8] for our system, for sand the occurrence of SOC is highly debated [9]. It is conceivable that a certain minimum amount of disorder is necessary for SOC behaviour to occur. This idea is supported by the experiments of Altshuler et al. on steel balls [19] and by some of us on superconductors [20], and may also explain why in the Oslo experiments [12], long grained rice (like ours) behaved as SOC while more rounded rice did not.

In experiments that started from a manually prepared 'flat' pile, we investigated the approach from this 'flat' state towards the SOC state. Again, within experimental accuracy, the scaling relation (17) is corroborated by our experiment. In the approach towards SOC, the avalanches are smaller and their distribution is steeper, making the chance for large avalanches much smaller than in the SOC state. It seems that the best strategy to avoid huge avalanches is to stay away from the SOC state. That is indeed possible by continuously disturbing the pile.

References

1. B. Gutenberg, C.F. Richter: *Seismicity of the Earth and Associated Phenomena* (Princeton University Press, Princeton 1949); B. Gutenberg, C.F. Richter: Bull. Seis. Soc. Am. **34**, 185 (1944) and B. Gutenberg, C.F. Richter: Ann. Geofis. **9**, 1 (1956)
2. K.W. Birkeland, C.C. Landry: Geophys. Res. Lett. **29**, 1554 (2002)
3. C.M. Aegerter: Physica A **319**, 1 (2003)
4. X. Gabaix, P. Gopikrishnan, V. Plerou, H.E. Stanley: Nature **423**, 267 (2003)
5. P. Bak, K. Sneppen: Phys. Rev. Lett: **71**, 4083 (1993)
6. P. Bak, C. Tang, K. Wiesenfeld: Phys. Rev. A **38**, 364 (1988)
7. P. Bak: *How Nature Works* (Copernicus, New York 1966)
8. M. Paczuski, S. Maslov, P. Bak: Phys. Rev. E **53**, 414 (1996)
9. H.M. Jaeger, S.R. Nagel, R.P. Behringer: Rev. Mod. Phys. **68**, 1259 (1996); S.R. Nagel: ibid. **64**, 321 (1992) and references therein
10. C.M. Aegerter, R.Günther, R.J. Wijngaarden: Phys. Rev. E **67**, 051306 (2003)
11. C.M. Aegerter, K.A. Lőrincz, M.S. Welling, R.J. Wijngaarden: Phys. Rev. Lett. **92**, 058702 (2004)
12. V. Frette, K. Christensen, A. Malthe-Sørenssen, J. Feder, T. Jøssang, P. Meakin: Nature **379**, 49 (1996)
13. A.L. Barabasi and H.E. Stanley: *Fractal Concepts in Surface Growth* (Cambridge University Press, Cambridge, 1995)
14. J. Schmittbuhl, J.-P. Vilotte, and S. Roux: Phys. Rev. E **51** (1995) 131; M. Siegert: ibid. **53**, 3209 (1996); J.M. Lopez, M.A.Rodriguez, R. Cuerno: ibid. **56**, 3993 (1997)
15. B.B. Mandelbrot: *The Fractal Geometry of Nature* (Freeman, New York 1983)

16. M. Kardar, G. Parisi, Y.C. Zhang: Phys. Rev. Lett. **56**, 889 (1986)
17. H.J. Jensen: *Self Organized Criticality* (Cambridge University Press, Cambridge 1998)
18. C.M. Aegerter, K.A. Lőrincz, R.J. Wijngaarden: Europhys. Lett. **67**, 342 (2004)
19. E. Altshuler, O. Ramos, C. Martinez, L.E. Flores, C. Noda: Phys. Rev. Lett. **86**, 5490 (2001)
20. M.S. Welling, C.M. Aegerter, R.J. Wijngaarden: cond-mat/0410369.